JOURNAL DE PHYSIQUE *Colloque* C4, *supplément au n°* 10, *Tome* 37, *Octobre* 1976, *page* C4-139

CHARGE DENSITY WAVES IN THE LAYERED TRANSITION METAL DICHALCOGENIDES

P. M. WILLIAMS

V. G. Scientific Ltd, East Grinstead, Sussex, U. K.

C. B. SCRUBY

Materials Physics Division, AERE Harwell, Didcot, Oxon, U. K.

and

W. B. CLARK and G. S. PARRY

Dept. Chemical Engineering and Chemical Technology
Imperial College, London, U. K.

Résumé. — Les dichalcogénides de métaux de transition de groupe V_a présentent une surface de Fermi reliable aux instabilités structurales. Dans des corps tels que IT-TaS_2, ces effets apparaissent clairement dans les propriétés électromagnétiques qui sont anormales. Le but de l'article est de présenter des preuves expérimentales, en particulier par la diffraction des électrons et les rayons X, pour l'adoption d'un état fondamental CDW couple a une distorsion périodique de réseau. Nous montrons comment cet état fondamental peut être perturbé en intercalant des métaux alcalins ou des terres rares.

Abstract. — The metallic layered transition metal dichalcogenides of group V_a exhibit Fermi surface linked structural instabilities. In materials such as IT-TaS_2, these effects readily manifest themselves in the electromagnetic properties, hitherto regarded as anomalous. The primary aim of the present paper is to present the diffraction evidence from electron and X ray observations, for the adoption of a charge density wave ground state coupled to a periodic lattice distortion, and to show how this ground state may be perturbed by alkali metal and rare earth intercalation.

1. **Introduction.** — Recent recognition [1, 2] that certain properties of the group V_a transition metal dichalcogenides (TMD), hitherto regarded as *anomalous*, might be interpreted in terms of an electronic instability, has stimulated considerable interest in these layered metals. Nominally of simple structure, related either to that of $CdCl_2$ ($P\bar{3}m$) or MoS_2 ($P\,6_3/mmc$), the earliest indications of such anomalous behaviour were reported in electron diffraction studies by Wilson and Yoffe (1968). For the octahedral polytype of TaS_2 (hereafter denoted 1 T-TaS_2), these authors found extra reflexions in (hk.0) projection diffraction patterns which were not anticipated for the space group $P\bar{3}m$; explanations in terms of either a shear structure or an excitonic insulator phase were offered at that time. Later, Thompson *et al.* [4] in studies of temperature dependence of the electrical conductivity of the same material found evidence of two first order phase transitions between states characterized most readily by their anomalously high resistivities. Their data for 1 T-TaS_2 is summarised in figure 1 together with that for 1 T-$TaSe_2$, and for the trigonal prismatically coordinated polytypes of the same materials (denoted 2 H-TaS_2 and 2 H-$TaSe_2$), as reviewed recently by Wilson *et al.* [2]. Over no range of temperature in figure 1 can the resistivity behaviour of 1 T-TaS_2 be classified as *metallic* even though simple charge transfer arguments (Wilson and Yoffe [3]) suggest metallic properties for all the group V_a TMD's. Indeed, detailed band structure calculations (Mattheiss [7]) and photoemission measurements (Shepherd and Williams [8] ; Smith *et al.*[31]) both show narrow « d » bands which contain one electron per formula unit for group V_a 1 T and 2 H polytypes. Further evidence for departures from simple metallic behaviour has been observed for most of the group V_a TMD's, as reviewed by Wilson *et al.* [2].

With reference again to 1 T-TaS_2, the behaviour in figure 1, particularly within the temperature range 190-350 K, is in fact more reminiscent of a semiconductor than a metal, as first pointed out by Thompson *et al.* [4] ; comparison with materials such as SmS, however, where f-d hybridization may result in the opening of an energy gap at the Fermi level, are clearly inappropriate in the present case. A closer analogue may be found in recent work on so called *one-dimensional* metals such as KCP (Comes *et al.* [9]) where the structures have been recognized for some time as inherently unstable below an appropriate temperature with respect to a Peierls Transition

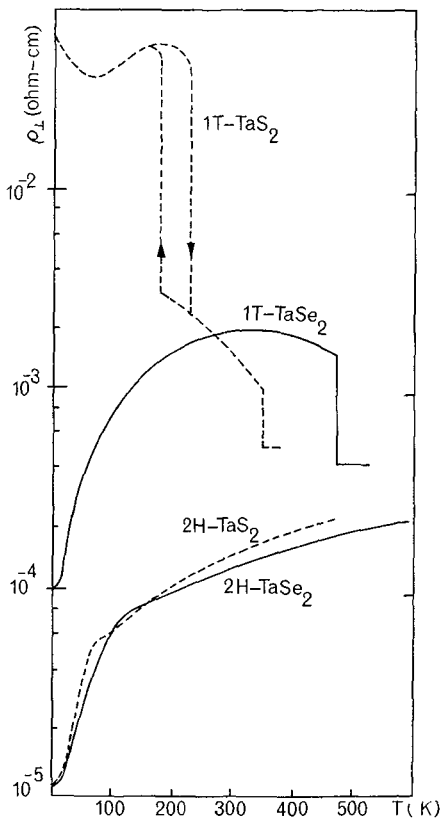

FIG. 1. — Resistivity parallel to the layer as a function of temperature for 1 T and 2 H tantalum dichalcogenides. Note indications of first order transition behaviour for the 1 T polytypes (from ref. [3]).

(Peierls [10]) to an insulating state. In this state, the creation of new Brillouin zone boundaries stabilized by periodic structural distortion of the lattice results in band filling and the creation of an energy gap at the Fermi level with a consequent lowering of the total energy of the system. Such a transition may be conveniently structurally characterized in terms of a phonon mode of appropriate wave vector (in this case parallel to the one-D axis) becoming *soft* i.e. tending, in the limit, to zero frequency. In this respect, further consideration of phonon-based anomalies in three dimensional metals is appropriate ; in particular, Kohn [11] predicted a softening of phonon modes with wave vector just sufficient to span the Fermi surface, from a consideration of the divergent contribution to the generalized susceptibility of the conduction electron gas. Such anomalies were later detected in the phonon spectra of simple metals such as lead (Brokhouse [12]). Overhauser [13] has extended these ideas to include the concept of a ground state for certain metals in which these density fluctuations in the electron gas (the *charge density wave* or CDW) are coupled to a periodic structural distortion of the lattice (a *periodic lattice distortion* or PLD) in a stable configuration. Although originally proposed with the alkali metals in mind, these ideas have quite general applicability, as is further discussed below.

Against the above background, electron diffraction observations in particular, of the superlattices and diffuse scattering observed as a function of temperature in the octahedral dichalcogenides of Tantalum led to the suggestion that these structural effects might themselves be driven by a giant Kohn-like anomaly, leading to a charge density wave ground state for the metallic layer TMD's (Williams *et al.* [1] ; Wilson *et al.* [2]). Since then, numerous structural and electromagnetic studies of these and related layer TMD's have been reported. Theoretical and electronic considerations of these phenomena are dealt with in detail elsewhere in the present proceedings. In the present paper, we will therefore confime ourselves to a detailed consideration of the structural aspects of the problem, particularly with reference to 1 T-TaS_2. This material may be regarded as both archetypal of this class of CDW/PLD ground state metals and, in certain respects, exceptional, in its exhibition of two incommensurate CDW phases. The following sections, then, will present the diffraction data for this and other TMD's. The consequences of doping and intercalation on the ground state structure will also be reviewed. Finally, we will attempt to indicate how these observations might be interpreted in terms of the currently accepted models for the electronic structure of these materials.

2. **Diffraction observations.** — The octahedral, 1 T polytypes related to the CdI_2 structure (P $\bar{3}$m) are most common amongst the $3d^1$ and $5d^1$ dichalcogenides of vanadium and tantalum, although DiSalvo and co-workers (1975) have reported the growth of 1 T crystals of $NbSe_2$ substitutionally doped with Ti. Here we will consider in detail the case of 1 T-TaS_2 as outlined above. This data will be contrasted with effects observed in the 2 H, trigonal prismatic polytypes of $TaSe_2$ and $NbSe_2$ (P 6_3/mmc) where the CDW/PLD ground state appears to adopt a different form. The contrast between 2 H and 1 T polytypes is further highlighted in observations of 4 H_b-TaS_2 where octahedral and trigonal prismatic layers alternate ; it will be shown that these layers apparently behave independently and conform to their parent (1 T or 2 H) lattice type. Controlled perturbation of the CDW/PLD ground state in the 1 T-polytypes will be demonstrated following electron transfer on doping or intercalation.

2.1 1 T-TaS_2. — Since the earliest report of *superlattice* effects in high energy electron diffraction patterns of 1 T-TaS_2 (Wilson and Yoffe [3]), extensive studies have been carried out by many groups using electrons and X rays (Wilson *et al.* [2] ; Williams *et al.* [1], [15]). Although there have been certain differences over the interpretation of results, there is an almost precise reproducibility between the diffraction patterns recorded over a wide range of temperatures for materials prepared in different laboratories. We reproduce in figure 2 the results of Scruby *et al.* [1] showing (hk.0) transmission electron diffraction

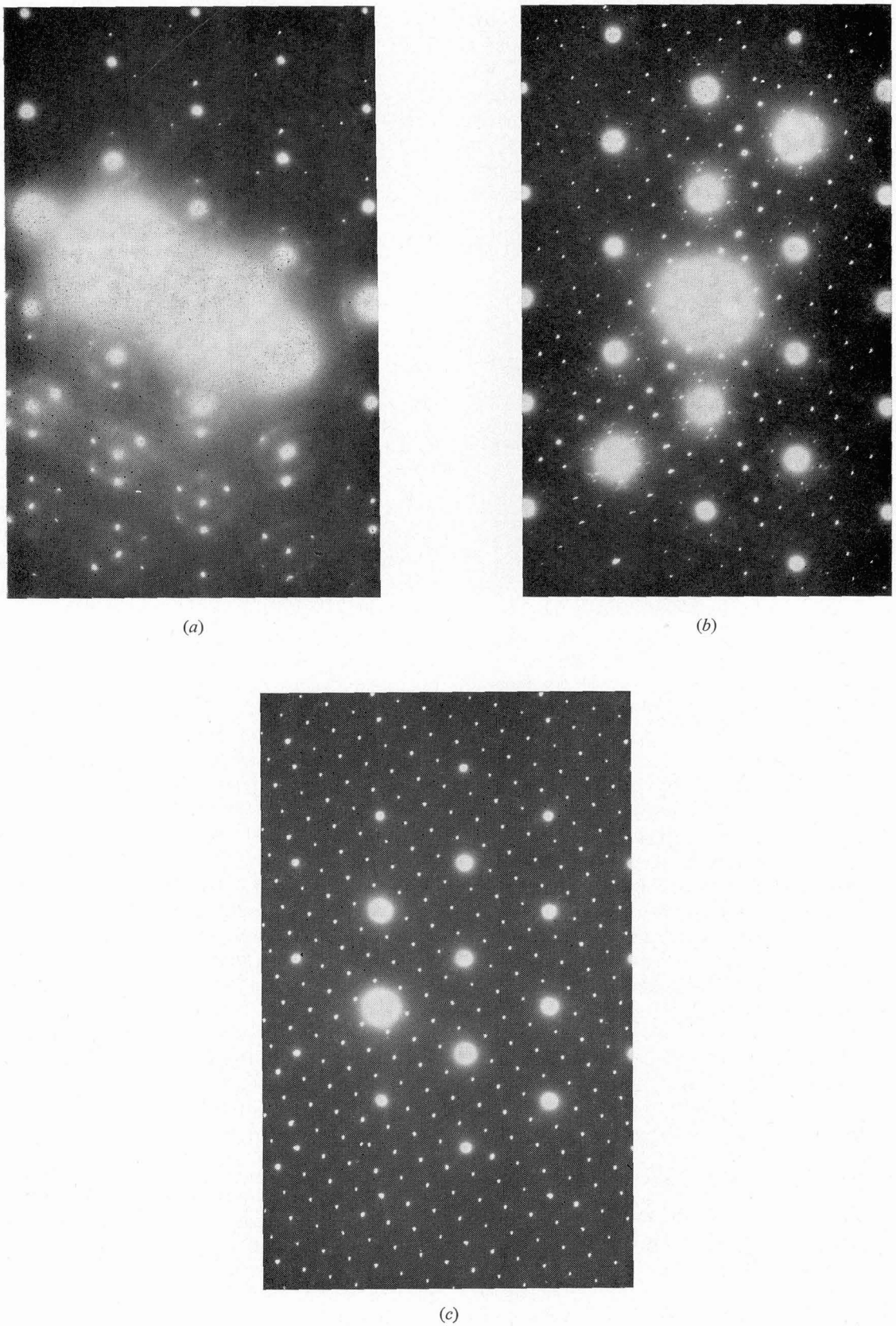

FIG. 2. — Selected area diffraction patterns for 1 T-TaS_2 with incident electron beam parallel to **c*** (a) the 1 T *phase* at 340 K showing strong triangular groupings $\{S_M\ (10.l)\}$; *b*) 1 T_2 at 290 K ; *c*) 1 T_3 at 150 K.

patterns for 1 T-TaS_2 recorded at the temperatures indicated (using either heated or liquid nitrogen cooled stages in a JEM 7A electron microscope operating at 100 keV). The three phases are denoted 1 T_1, 1 T_2 and 1 T_3 (after Williams *et al.* [1]) to indicate regions in the $\rho \rightarrow T$ relationship of figure 1 above the first transition, between first and second transitions, and below the second transition in temperature respectively. The transformation temperature of the 1 T_3 phase we will denote T_d (after Wilson *et al.*) that from 1 T_1-1 T_2, T_d'. Figure 3 reproduces single crystal X-ray oscilla-

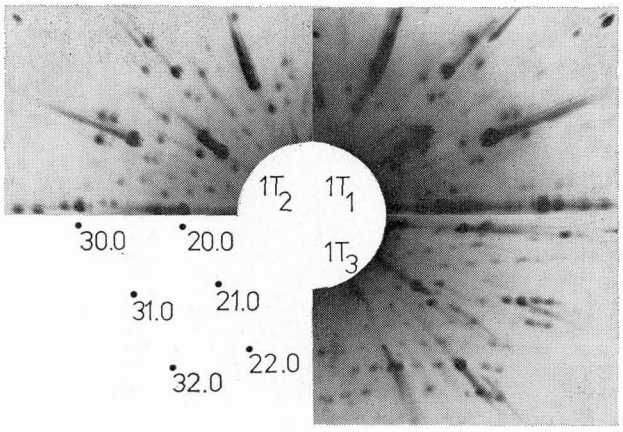

FIG. 3. — Oscillation X-ray photographs with incident beam in similar orientation to figure 2 for (*a*) 1 T, at 390 K (*b*) 1 T_2 at 290 K (*c*) 1 T_3 at 80 K confirming the reciprocal space geometry given by electron diffraction. Distortion amplitude is too small in 1 T_1 for S_M (11.*l*) to be observed.

tion photographs (Scruby *et al.* [2]) again for the three regimes 1 T, 1 T_2, 1 T_3. With both X-ray and electron diffraction, the extra periodicities refered to above, which are not consistent with the simple CdI_2 structure, are clearly noted, the X ray observations confirming that these periodicities seen perhaps most readily in selected area diffraction are characteristic of bulk single crystals and not of localized defects. For convenience, we summarize this data schematically in figure 4 ; thus the matrix CdI_2 structure reflexions, { **M** }, are surrounded by groups of extra reflexions, { $\mathbf{S_M}$ }, disposed with three or six fold symmetry about each *parent* in { **M** }. If vectors $\mathbf{Q}_{in}$ (where *i* refers to a set of 3 symmetry related PLD's and 1 T_n for $n = 1, 2$ or 3 the region of the $\rho \rightarrow T$ curve, Fig. 1) define the disposition of the { $\mathbf{S_M}$ } about each { **M** } as shown then the following may be deduced for the three *phases*.

a) In both 1 T_1 and 1 T_2 the magnitude of vectors $\mathbf{Q}_{in}$, $|\mathbf{Q}_{in}|$, defining the first order reflexions in { $\mathbf{S_M}$ }, is an irrational fraction of the reciprocal lattice parameter of matrix structure, $|\mathbf{a}^*|$. Only in 1 T_3 do $\mathbf{Q}_{i3}$ and $\mathbf{a}^*$ become *commensurate* (i.e. they are related on a rational coincidence mesh), the { $\mathbf{S_M}$ } defining in the (hk.0) plane a perfect $\sqrt{13} \times \sqrt{13}$ superlattice mesh.

b) The vector $\mathbf{Q}_{i1}$ in 1 T_1 is parallel to $\mathbf{a}^*$ but rotates by 110° 6′ away from $\mathbf{a}^*$ at the transition to

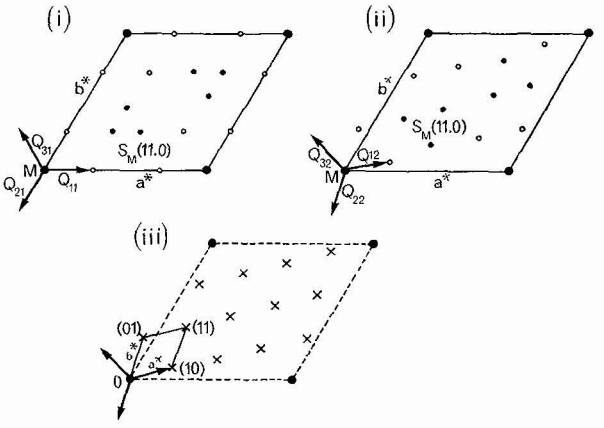

FIG. 4. — Reciprocal cells for each distorted 1 T-TaS_2 phase, where $\mathbf{Q}_{i1}$, $\mathbf{Q}_{i2}$, $\mathbf{Q}_{i3}$ are distortion wave vectors. In (*a*) 1 T_1 and (*b*) 1 T_2 the unit cell is that of the matrix with : — { $\mathbf{S_M}$ } reflexions in (*hk*.0) plane of { **M** } ; — { $\mathbf{S_M}$ } reflexions at $\pm \frac{1}{3}\mathbf{c}^*$. In (c) 1 T_3, the commensurate distortions define a reduced $\sqrt{13} \times \sqrt{13}$ reciprocal cell, shown in projection.

1 T_2. $\mathbf{Q}_{i2}$ then rotates gradually, as the temperature is lowered, to ~ 14° at the transition to 1 T_3 to form the perfect $\sqrt{13} \times \sqrt{13}$ superlattice. At the same time $|\mathbf{Q}_{i2}|$ varies in magnitude with temperature, decreasing from 0.286 a^* at T_d' to 0.277 a^* at T_d.

c) Second order reflexions of the type $\mathbf{Q}_{12} \pm \mathbf{Q}_{22}$ are observed in both 1 T_1 and 1 T_2 (and of course in the perfect superlattice mesh of 1 T_3), being most noticeable in 1 T_2 (Fig. 2). Following the notation of Scruby *et al.*, we will adopt a system of coordinates local to each { **M** } to describe the association { $\mathbf{S_M}$ } ; thus the first order reflexions we will denote $\mathbf{S_M}$ (10.*l*) the second $\mathbf{S_M}$ (11.*l*). This notation will be used throughout the text in the descriptions of all the materials.

d) Within the 1 T_1 phase, in addition to the { $\mathbf{S_M}$ }, there is a diffuse background in the form of streaks passing through the $\mathbf{S_M}$ (10.*l*) apparently in the form of *circles* or *bicycle chains* (Wilson *et al.* [2]). The intensity in these streaks increases with temperature until the irreversible 1 T-2 H inter-polytypic transition occurs near 450 K ; figure 5 shows a typical higher-temperature transmission electron diffraction pattern accentuating this streaking ; the precise interpretation of this effect is the subject of some controversey, as we shall see later.

These results for 1 T-TaS_2 establish the basic characteristics of the observations, many of which are common to other layer materials within the group. In particular, 1 T-$TaSe_2$ exihbits similar diffraction effects, with the exception that the intermediate, 1 T_2 phase is absent. Thus we shall see that in many respects, the incommensurate nature of the $\mathbf{Q}_{i1}$, at high temperature ($> T_d$) is the *signature* of the charge density wave in the electron gas, being related to the geometry of the Fermi surface and not of the lattice. The diffracted intensities derive, however, not from the scattering

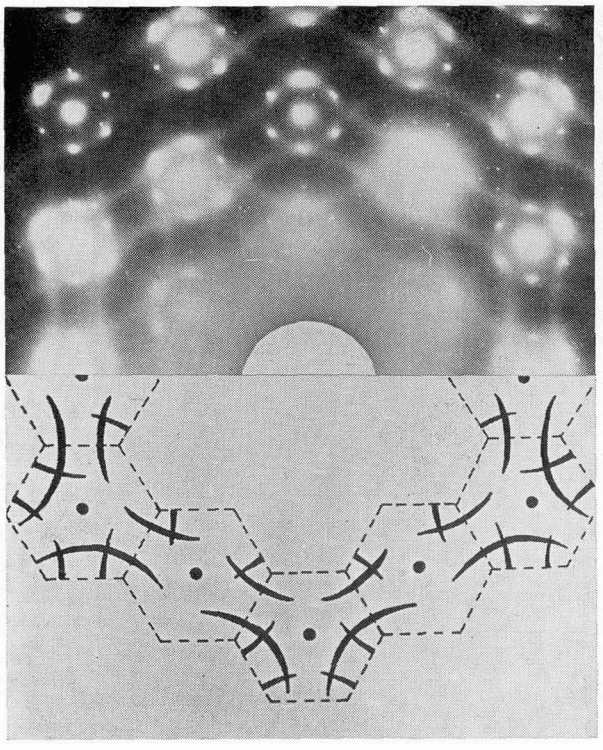

FIG. 5. — Selected area electron diffraction pattern for 1 T_1-TaS_2 at 420 K showing diffuse streaking which images the Fermi surface. All six $\{ S_M(10.1) \}$ reflexions are visible because of crystal buckling.

from the maxima in this CDW (this produces a negligible contribution) but from the associated PLD. Here the effects in diffraction space are less open to question in that the intensity variations in the $\{ \mathbf{S_M} \}$ for increasing h, k indices in M($hk.0$) may be predicted exactly (section 3 below). For the present, we will note that in figure 6, which reproduces an MoKα oscillation photograph with the X-ray beam incident perpendicular to c*, the intensities in the $\mathbf{S_M}$ ($10.l$) (rows arrowed) increase dramatically as we pass from **M** ($00.l$), ($0.1l$), through **M** ($10.l$), ($11.l$), to **M** ($20.l$), ($21.l$). This intensity variation, as has been pointed out by Comes [9] and others in the related case of the one dimensional metals, is very specifically the *signature* of a periodic modulation of the lattice and *cannot* be explained in terms of defect ordering or shear structures, as originally proposed. This X-ray observation is thus, along with the neutron data for the 2 H polytypes (Monckton *et al.* [15]), the single most conclusive piece of evidence for CDW/PLD behavior in these materials. The intensities in the electron observations again show similar increases for $\mathbf{S_M}$ ($10.l$) with increasing M($hk.0$), but in this case, curvature of the Ewald sphere in reciprocal space precludes too literal an interpretation of the variations. Again with reference to figure 6, careful study shows the reflexions $\mathbf{S_M}$ ($10.l$) to be located out of the ($hk.l$) planes at positions $= \pm$ c*/3, forming an octahedron of reflexions about each $\{ \mathbf{M} \}$, of local symmetry $\bar{3}$ (a fact which may also be deduced from careful electron microscope observations by tilting flat areas of sample). This observation is true for both 1 T_1 and 1 T_2 phases and implies strong correlation between PLD's in neighbouring layers ; the situation in 1 T_3 is more complex and is discussed fully below. Finally, with reference to TaS_2, we note that in both the 1 T_1 and 1 T_2 phases, the matrix appears to remain strictly hexagonal ; in 1 T_3, there is some indication that this is no longer true, the structure being triclinic with a stacking repeat of 13 c^0 as opposed to 3 c^0 in 1 T_1 and 1 T_2.

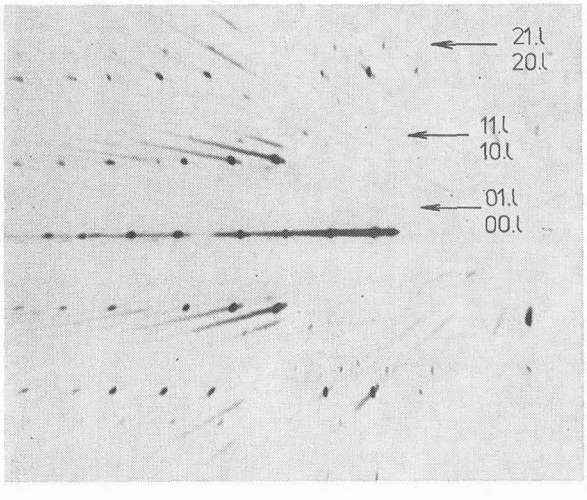

FIG. 6. — Oscillation X-ray photograph of 1 T_2-TaS_2 with incident beam perpendicular to c*, and recorded with a cylindrical camera. There is an increase in intensity of $\{ \mathbf{S_M} \}$ reflexions (indicated by arrows) relative to the adjacent matrix reflexions with increase in the component of scattering vector normal to c* (M($0\,k.l$) to M($1\,k.l$) to M($2\,k.l$)).

2.2 THE 2 H POLYTYPES : $NbSe_2$ AND $TaSe_2$. — Figure 1 presents much less dramatic evidence, in the form of weak shoulders in the T data, for electronic anomalies in the 2 H polytypes of the metallic layered TMD's, although examination of the same temperature region with other forms of physical measurement (e.g. magnetic susceptibility, Wilson *et al.* [2] ; elasticity, Barmatz *et al.* [16]) does reveal anomalous discontinuities. Equally, early structural studies at room temperature (Wilson and Yoffe [3]) using electron diffraction revealed no extra scattered intensity, but low temperature magnetic resonance studies $NbSe_2$ (Ehrenfreund *et al.* [17]) suggested Niobium site inequivalencies, and low temperature X-ray diffraction (Marezio *et al.* 1972) again demonstrated the possibilities of some weak distortion. More recently, direct evidence of a low temperature structural distortion in the 2 H polytypes has been obtained from both electron (Williams *et al.* [15]) and neutron (Monckton *et al.* [15]) diffraction and from n.m.r. data (Valic *et al.* [18], Berthier *et al.* [18]). The electron data is reproduced in figure 7 which shows ($hk.0$) diffraction patterns recorded at 40 K for $TaSe_2$ and 17 K for $NbSe_2$. In neither case could any relexions other than

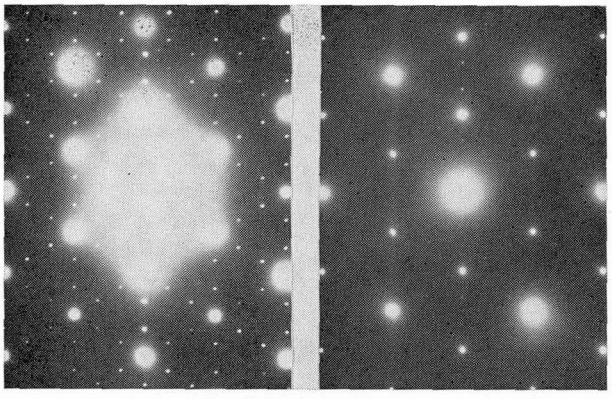

FIG. 7. — (*hk*.0) selected area electron diffraction patterns for (a) 2 H-$TaSe_2$ at 40 K, with $\mathbf{Q}_i$ now commensurate at $\pm \frac{1}{3}\mathbf{a}^*$ and showing second order $\{S_M\ (11.0)\}$ reflexions. (*b*) 2 H-$NbSe_2$ at 17 K, showing sharp $\{S_M\ (10.0)\}$ reflexions with $\mathbf{Q}_i$ incommensurate ($< \pm \frac{1}{3}\mathbf{a}^*$). Note the $\{S_M\}$ are weak when $\{M\}$ is strong for $h - k = 3n$, indicating antiphase PLD's in Nb and Se layers.

the matrix M be observed at room temperature, but for $TaSe_2$, cooling to around 100 K reveals the build up in scattered intensity S_M close to but not coincident with $+ a^*/3$. For $NbSe_2$, this build up is not observed until below 33.5 K (Williams *et al.* [15], Monckton *et al.* [15]). In both cases, the deviation, from the commensurate position is small (1-2 %), but whilst for $TaSe_2$, a transition to a commensurate state occurs near $T_d = 90$ K, $NbSe_2$ remains incommensurate down to 5 K. Thus in figure 7, weak second order reflexions S_M (11.0) define, with the first order S_M (10.0) a perfect 3 × 3 superlattice for 2 H-$TaSe_2$, whereas for $NbSe_2$, no second order reflexions can be detected, even after prolonged exposure. In neither case could tilting of the crystal reveal any significant modulation of scattered intensity // $\mathbf{c}^*$ for the S_M indicating little or no phase coherence in the PLD's in neighbouring layers although the n.m.r. data (Berthier *et al.*) would seem to indicate a static well correlated mode. Monckton *et al.* [15] have fully analysed and discussed the distortion modes present in the 2 H polytypes. For the present, we note that qualitatively, there are considerable dissimilarities between the PLD effects in the 1 T and 2 H materials, in terms of the temperature ranges over which the effects are observed, the magnitudes and directions of the wave vectors $\mathbf{Q}_{in}$ defining the disturbance, and the intensity dependence in the $\{S_M\}$ with temperature. The projected forms of the Fermi surface for 1 T and 2 H polytypes do differ, in fact, but the scale of the dissimilarities between the two groups in their PLD behaviour has led to suggestions that quite different mechanisms may be responsible for the lattice distortions within the two, as is discussed elsewhere in the present proceedings (Rice, *ibid.*, 1976). Finally, we note that observations of 2 H-NbS_2 down to 10 K have revealed no trace of extra scattering, consistent with the absence over a similar temperature range of any electronic anomalies for this material (Forgan, private communication).

2.3 MIXED POLYTYPES : 4 H_b-TaS_2. — The above contrast in behaviour between 1 T and 2 H polytypes raises interesting questions regarding the behaviour to be expected for mixed polytypes such as 4 H_b-TaS_2. This material comprises alternating layers with octahedral and trigonal prismatic coordination of the Ta by S. As such, effects related to both classes of phenomena considered above might be anticipated. Both resistivity (Wattamaniuk *et al.* [20]) and susceptibility data (Wilson *et al.* [2]) reveal evidence for first order transitions near 315 K and 20 K, and it has long been conjectured that the upper of these derives from CDW/PLD behaviour in the octahedral layers, the lower one from the trigonal prismatically coordinated layers. This is in contrast to the case of 1 T-TaS_2 where both upper and lower transitions (T_d' and T_d) must clearly be associated with octahedral layers only. Once more, recent evidence from both neutron (Di Salvo *et al.* [21]) and electron (Tatlock [22]) diffraction provides an answer. Figure 8 shows an (*hk*.0) transmission electron diffraction recorded at 14 K from a single crystal of 4 H_b-TaS_2 prepared by annealing a parent crystal of 1 T-TaS_2. The apparently complex diffraction pattern may be decomposed into three contributions, two of which represent symmetry equivalent $\mathbf{a}\sqrt{13} \times \mathbf{a}\sqrt{13}$ superlattices, such as is observed

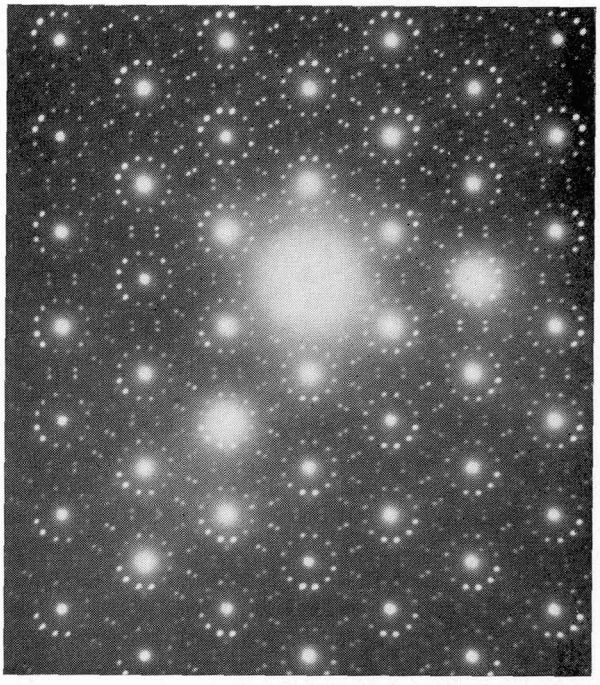

FIG. 8. — (*hk*.0) selected area electron diffraction pattern for 4 H_b-TaS_2 at 14 K, showing two orientations of a perfect $\sqrt{13} \times \sqrt{13}$ superlattice in the octahedral layers and, much weaker near $\pm \mathbf{a}^*/3$, corresponding to PLD's in the trigonal prismatic layers (after Tatlock).

in 1 T_3-TaS_2. The third contribution, consisting of weaker reflexions close to, but not coincident with $\pm$ **a***/3, may readily be compared with the data of figure 7 for the 2 H polytypes ; this third set of reflexions $\{ S_M \}$ remains incommensurate down to 10 K. No absolute support may as yet be derived from accurate structure factor fits to the measured intensities in either neutron or electron studies, but nevertheless, the inescapable conclusion in the present case is that the $\sqrt{13} \times \sqrt{13}$ superlattice is located only within the octahedral layers, the incommensurate distortion only within those with trigonal prismatic coordination. This is perhaps the most striking example of two dimensionality in these layered solids, the two types of layers behaving effectively independently. Such is their apparent independence that Wattamaniuk *et al.* [20] have suggested that the transport properties *c* for this material may be considered in terms of tunnelling between metallic (trigonal prismatic) layers separated by insulating (octahedral) layers.

2.4 Diffraction Studies of Interealated Materials. — The effects described above in the pure, stoichiometric materials will be discussed in section 3 in terms of charge density wave instabilities. For the present, we suggest only that these structural anomalies are related in some way to the Fermi surface in these materials ; their behaviour following controlled changes in the size of shape of the surface should therefore be regarded as one of the most significant tests of this hypothesis. Within the layered compounds, such changes may readily be accomplished in one of two ways. Substitutional doping of the cation enables continuous variation in electron density to be produced, provided that it is possible to grow single phase crystals of such mixed compounds. Alternatively, the layered compounds offer a unique means of controlling the intralamellar electron density via intercalation, that is the insertion between lamellae of dopant species such as alkali metals and organic compounds, notably the amines. Wilson, Di Salvo, and co-workers have extensively investigated the electronic properties and structures of doped group $\overline{V}_a$ TMD's, as considered elsewhere in the present proceedings (Di Salvo). For the present we note only that whilst it is relatively easy to control the overall electron density and hence the size of the Fermi surface in 1 T-TaS_2, for example, by the substitution of Ti, the random cation potentials so introduced tend to scatter the charge density wave and hence introduce disorder into the PLD effects observed in diffraction. Such scattering favours the adoption of an incommensurate CDW/PLD ground state, as pointed out by McMillan [23], thereby preventing the controlled study of new commensurate superlattice structures (Wilson *et al.* [2]).

With regard to the individual lamellae on the other hand, intercalation can be considered as less disruptive. The intercalating or *guest* species often orders on some lattice array determined by, and hence commensurate with the host lattice. As such, although these species may be charged, no new Fourier components are introduced into the modified crystal potential with which the CDW interacts. Furthermore, the CDW, which may be regarded as having existence predominarily within the layer, may be effectively screened from any new potentials introduced by the regular ionic array in the interlamellar space, thereby again minimising scattering. Since electron transfer to the host layer is thought to accompany intercalation (see, for example, Acrivos *et al.* [24]) this method has many attractions as a controlled means of studying the consequences of Fermi surface expansion for the CDW/PLD ground stage.

For 1 T-TaS_2, the alkali metals Li, Na, K and the rare earth Europium have all been successfully intercalated, either from solution in ammonia (Na, K, Eu) or, for Li, from n-butyl lithium (Clark *et al.* [25]). Figure 9*a* shows the diffraction pattern which results at

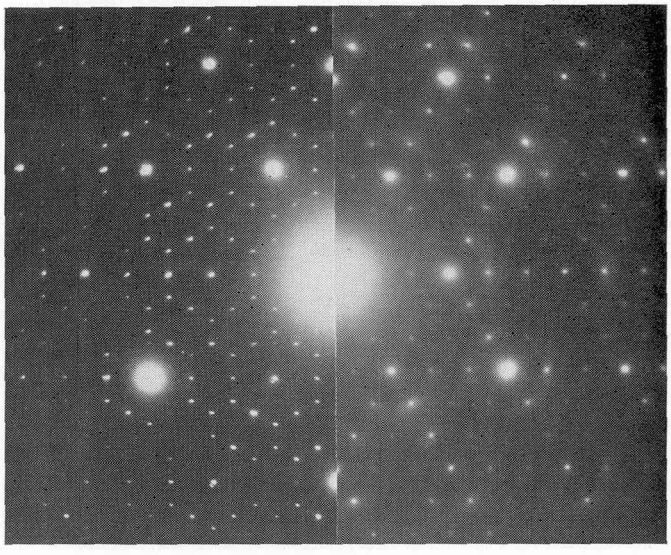

Fig. 9. — (*hk*.0) selected area electron diffraction patterns for (*a*) 1 T-TaS_2 intercalated with Na, 295 K and (*b*) the same, at 100 K. Pattern (*a*) was also obtained for K, Li and Eu intercalates.

room temperature following saturation intercalation. In each case, a geometrically identical pattern is produced, independent of the metal used, strongly suggesting that the diffraction effects are associated with the TaS_2 layer and not with the intercalate (Lithium, for example, has insufficient scattering power for electrons or X-rays to account for the present observations). X-ray diffraction data yields similar results and figure 10 shows a crystal of Li_x1 T-TaS_2 recorded at room temperature (W. B. Clark, unpublished). The same cell as in figure 9*a* is observed confirming the bulk nature of these effects. This apparently complex pattern may in fact be interpreted in terms of two PLD's ($\mathbf{Q}_i^1 = \pm$ **a***/3 ; $\mathbf{Q}_i^2 = \pm (2$ **a*** $\sqrt{3})/9)$ suggesting some competition on the Fermi surface for the optimum

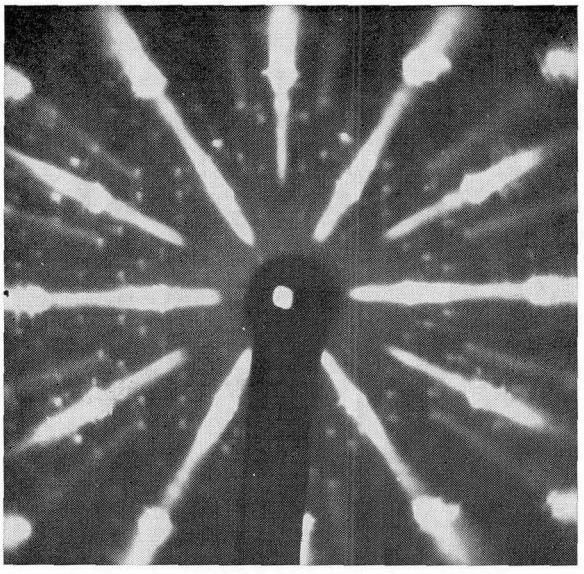

FIG. 10. — Oscillation X-ray photograph corresponding to figure 9, for *Li* intercalated 1 T-TaS_2, recorded at 295 K.

spanning vector Lowering the temperature, however (Fig. 9*b*) produces an interesting transition to a state in which $\mathbf{Q}_i^2$ is absent, the remaining reflexions forming a perfect 3 × 3 superlattice. Detailed discussion of these effects is beyond the scope of the present paper. Here, we confine ourselves to noting that the wave vectors characterizing the PLD do expand on intercalation relative to those in pristine 1 T-TaS_2 consistent with a change in size of the Fermi surface.

3. **Discussion.** — An interpretation of the above diffraction phenomena in terms of periodic lattice distortions and the origins of the latter in terms of charge density wave instabilities has been indicated where appropriate throughout the text. In this section, we will attempt to establish first the structural lines of this assertion and then to justify its further relationship to the electronic structures of these materials.

3.1 DIFFRACTION BY A DISTORTED STRUCTURE. — Readers are referred to standard texts for detailed consideration of the diffraction of electrons and X-rays (or neutrons) by periodically modulated structures. Here we will emphasise only the key features to be anticipated for such data. Assuming for the present, then, that distortion waves may be responsible, we note that for each of the hexagonal materials considered here, the trigonal (or hexagonal) disposition of the $\{ \mathbf{S_M} \}$ about $\{ \mathbf{M} \}$ implies the presence of three symmetry related distortions of wave vector $\mathbf{Q}_i$ and amplitude $\mathbf{U}_{Qi}$ where $i = 1, 2, 3$. The layered structures of all the materials suggests that the distortion waves lie within each layer so that $\mathbf{Q}_{in}.\mathbf{c}^* = 0$. This restriction on the orientation of $\mathbf{Q}_{in}$ implies that the Fourier transform of the distortion wave system within a single layer is a family of rods in reciprocal space, which are perpendicular to the layer and hence $\parallel \mathbf{c}^*$. The relative phases of the distortion waves in adjacent layers modulates these rods so as to produce sharp extra reflexions $\{ \mathbf{S_M} \}$ where $\{ \mathbf{M}=\mathbf{ha}^*+\mathbf{kb}^*+2\,\mathbf{c}^* \}$ is the scattering vector of a single reflexion in $\{ \mathbf{M} \}$ and $\mathbf{K} = \mathbf{M} + \mathbf{Q}_{in}$, the scattering vector of any extra reflexion in $\{ \mathbf{S_M} \}$.

Theories of the scattering of X-rays, electrons, or neutrons from regular lattices to which a periodic modulation has been applied are to be found elsewhere (see, for example, James [26] ; Overhauser [13]). Briefly, then, for the present case of three symmetry related distortions, the intensity of a matrix reflexion M will be reduced by a factor

$$1 - \sum_i (\pi \mathbf{M}.\mathbf{U}_{Qin}) ,$$

where $\mathbf{U}_{Qin}$ is the amplitude of the distortion mode $\mathbf{Q}_{in}$. More readily noted are the six first order reflexions $\mathbf{S_M}$ (10.2) with intensities proportional to

$$\tfrac{1}{4} \left| 2\,\pi(\mathbf{M} + \mathbf{Q}_{in}).\mathbf{U}_{Qin} \right|^2$$

at

$$\mathbf{M} \pm (\mathbf{Q}_{in} + n\,2\,\mathbf{c}^*) .$$

Strictly these expressions hold only when

$$(\mathbf{M} + \mathbf{Q}_{in}).\mathbf{U}_{Qin} \ll 1/2\,\pi ,$$

being approximations of Bessel functions

$$J_0(2\,\pi \mathbf{M}.\mathbf{U}_{Qin})$$

and

$$J_1(2\,\pi(\mathbf{M} + \mathbf{Q}_{in})) .$$

$\mathbf{U}_{Qin}$, which give the true intensities for $\{ \mathbf{M} \}$ and $\{ \mathbf{S_M} \}$ respectively. Nevertheless, since the approximation is valid for a distortion amplitude small compared with the lattice spacing for the first few orders in $\{ \mathbf{M} \}$, it is of use in considering the present results. Again, the above relates to a simple system with one atom per unit cell, but for TaS_2, where the scattering amplitude of the Ta atoms in the unit cell is considerably greater than that of the two sulphurs, we may apply the analysis directly. With the diselenides of Ta and Nb, the selenium now contributes significantly to the observed scattering, so we must now take into account the distortion waves in the chalcogen layers as well as in the cation sheets. However, this leads to extra information concerning the relative phases of these two sets of distortion waves, as is seen in 2 H-$NbSe_2$, for example.

3.2 THE 1 T POLYTYPES. — The distortion waves in 1 T-TaS_2 have been described in details by Scruby *et al.* [27]. For the present purposes, we will summarize their findings, noting firstly that for a given wave vector $\mathbf{Q}_{in}$, there are three possible distortion modes within the TaS_2 layer :

i) Longitudinal (LA) ; $\mathbf{U}_{Qin} \parallel \mathbf{Q}_{in}$ and $\perp \mathbf{c}^*$.
ii) Transverse (TA) ; $\mathbf{U}_{Qin} \perp \mathbf{Q}_{in}$ and $\perp \mathbf{c}^*$.
iii) Transverse (TA) ; $\mathbf{U}_{Qin}$ $\mathbf{Q}_{in}$ and $\parallel \mathbf{c}^*$.

By virtue of the dot vector product in the intensity expressions above, we may readily deduce which mode contributes predominantly. The increase in intensity in figure 6 of the $\{ \mathbf{S_M} \}$ surrounding each $\mathbf{M}(hk.l)$ for increasing h, k is expected for the increase in $(\mathbf{M} + \mathbf{Q}_{in})$ and thus confirms the supposition of a periodic distortion. Furthermore, since the $\{ \mathbf{S_M} \}$ increase in intensity with h, k but *not* significantly with 2 for any fixed row in reciprocal space, it must be concluded that $\mathbf{U}_{Qin} . \mathbf{c}^* = 0$, the distortions lying predominantly within the layers, as assumed above. Since the $\{ \mathbf{S_M} \}$ are also strongest for $\mathbf{Q}_{in} \parallel \mathbf{M}$ and weakest for $\mathbf{Q}_{in} \perp \mathbf{M}$, $\mathbf{U}_{Qin}$ must have a large component parallel to $\mathbf{Q}_{in}$ so that the distortions are predominantly LA.

The amplitudes of the distortion wave in the 1 T_2-TaS_2 structure is sufficient ($\sim$ 0.1 Å) to produce considerable intensity in the $\mathbf{S_M}$ $(10.l)$ reflexions ; for this case, it is then possible in the electron microscope to form a dark field image of the distortion wave as is shown in figure 11 (Scruby [27]) where one of the three

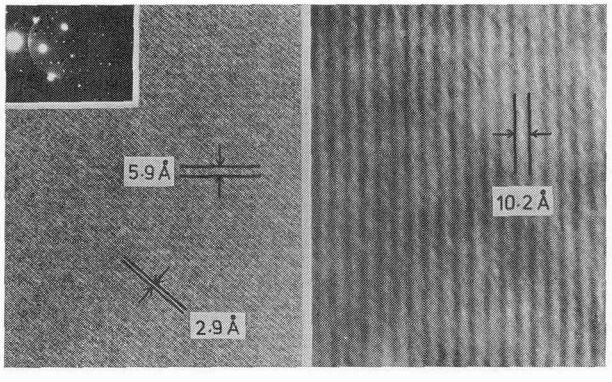

FIG. 11. — Dark field lattice electron micrograph of PLD in 1 T_2-TaS_2, formed from one of the $\{ \mathbf{S_M} (10.l) \}$ for M (20.0) (after Scruby).

symmetry related wave vectors $\mathbf{Q}_{in}$ and a matrix M (20.0) reflexion have been used. This observation, apart from high lighting the physical reality of these effects, assumes great value in the absence of neutron diffraction data for this material. Although electron and X-ray diffraction are inherently incapable of distinguishing between static and dynamic effects, the micrograph of figure 11 (with an exposure time of over 60 s) retains phase information and conclusively demonstrates this mode in 1 T_2 to be *soft* ; any fluctuations must be limited in amplitude to considerably less than the PLD wavelength, as any significant non zero frequency component would prelude its direct lattice imaging. The value of this result lies in its demonstration of the existence of long range static correlations in the incommensurate phase, since both diffraction data and the direct (averaged) measurement of PLD fringe spacing confirm the incommensurate nature of the mode. With regard to the differentiation between static and dynamic effects, it is also relevant here to point to the suggested dynamic origins of the diffuse streaking present in 1 T-TaS_2 (Scruby *et al.* [27]). For the present, we will not comment in detail on the appearance of this scattering except to identify (after Scruby *et al.*) the streaks as being predominantly transverse in character.

3.3 THE 2 H POLYTYPES. — Qualitatively the behaviour, in terms of PLD/CDW, differs considerably in the 2 H polytypes from that in the 1 T forms above. The lower temperatures at which the effects manifest themselves coupled with the thermodynamic stability of the 2 H trigonal prison coordinating unit, facilitates observation of the onset of the incommensurate phase in the undistorted metal ; this contrasts with the 1 T polytypes where irreversible transitions to the 2 H phase usually set in before this can be observed ($T \sim$ 400-600 K). The distortion wave amplitudes are considerably less in the 2 H forms and in all cases, the observations indicate that the extra reflexions $\{ \mathbf{S_M} \}$ are located with finite intensity within the zero layer in reciprocal space, suggesting the most likely interpretation in terms of a stacking repeat in phase with the matrix. Monckton *et al.* have shown in quantitative studies of $TaSe_2$ at 5 K that the static distortions in this material reveal opposite displacements of Ta and Se atoms. The electron observation of 2 H-$NbSe_2$ reinforces this argument (Fig. 7) where for reflexions where scattering from the Nb and Se atoms in the all reinforce (for $h - k = 3n$) leading to strong $\{ \mathbf{M} \}$, the associated $\{ \mathbf{S_M} \}$ are weak suggesting antiphase contributions from the PLD's in Nb and Se layers. For $TaSe_2$, $f(\mathrm{Ta}) \sim f(\mathrm{Se})$ so that this effect is not as readily observed. The distortion modes responsible for the $\{ \mathbf{S_M} \}$ are thus predominantly longitudinal in both 1 T and 2 H forms, although by and large, this is the only point of similarity between the two classes of polytypes.

3.4 ELECTRONIC ORIGINS OF THE LATTICE DISTORTIONS. — The reader is referred elsewhere for detailed considerations of the electronic origins of the above effects. Briefly, however, the response of a system of conduction electrons in a metal to an applied spatial perturbation of wave vector q is determined by the form of the renormalised susceptibility, χq, derived from the bare unscreened $\chi^0 \mathbf{q}$, where,

$$\chi^0 \mathbf{q} = \sum_{K} \frac{f_k - f_{k+q}}{E_{K+q} - E_k}$$

f_k, f_{k+q} being Ermi distributions over $| \mathbf{k} >, | \mathbf{k} + \mathbf{q} >$ of energies E_k, E_{k+q}. For a free electron, gas Kohn (1959) pointed out that as a result of the form of the denominator in the above, a logarithmic divergence in the static susceptibility $\chi^0 \mathbf{q}$ may occur when $\mathbf{q}$ is close to spanning the Fermi surface i.e. $\mathbf{q} \sim 2 \mathbf{k}_f$, giving rise to *Kohn anomalies* in the phonon spectra of metals. The magnitude of this effect is determined partly by the pricise Geometric form of the Fermi surface ;

and in particular Afanaseev *et al.* (1963) and later Fehlner and Loly [30] considered the increased contributions to the divergence in χ^0 **q** from cylindrical and nearly flat (i.e. parallel or *nesting*) pieces of Fermi surfaces, compared with the spherical surface discussed by Kohn.

If electron-electron as well as electron-phonon interactions are then taken into account, Overhauser [13] further postulated that below a suitable temperature, the divergence in χ^0 **q** may lead to the adoption of a CDW ground state in which the spatial fluctuations in electron density are determined by the $2\,\mathbf{k}_f$ wave vector. The CDW ground state is then stabilized by coupling to a PLD, the ion core displacements essentially screening out the inhomogeneities in the electrostatic field of the CDW. The lowering in electrostatic energy in the conduction electrons is thus balanced by the increased elastic strain energy of distortions in the lattice.

Against this background, the adoption of a CDW/PLD ground state, particularly in the 1 T polytypes, becomes a credible proposition. Figure 12

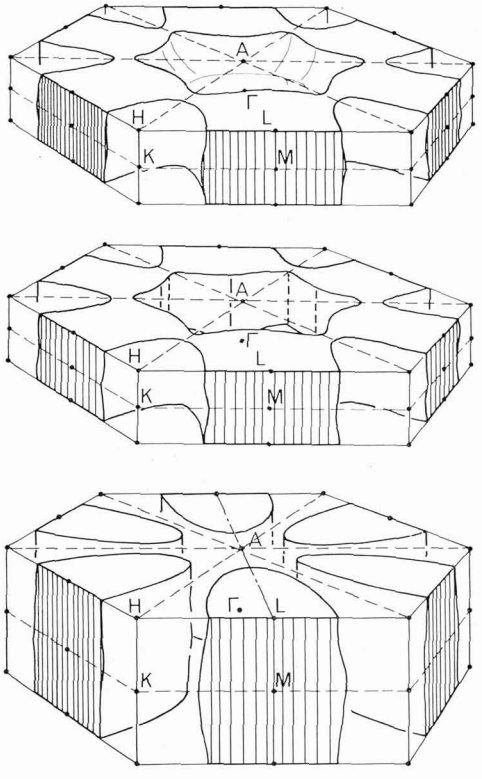

FIG. 12. — Fermi surfaces for (*a*) 2 H-TaS_2 showing both lower and upper bands respectively, deduced from the calculations of Mattheiss (*b*) 1 T-TaS_2.

reproduces the Fermi surfaces predicted for 2 H and 1 T-TaS_2 by Wilson *et al.* [2] from the calculations of Mattheiss [7]. Weak interlayer interactions, implying little band dispersion along **c***, result in large flat areas of Fermi surface, closely satisfying the criteria for good nesting. Empirically, figure 13 then compares the measured values (Scruby *et al.* [1]) of spanning vectors

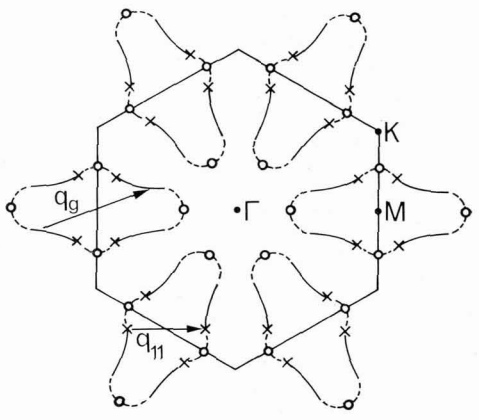

FIG. 13. — Comparison of, *x*, measured vectors $\mathbf{Q}_{i1}$ for 1 T-TaS_2 with, o, k_f values inferred from APW calculations, projected onto the ΓMK (*hk*.0) plane. Solid lines indicate part of surface *imaged* in diffraction by phonons.

$\mathbf{Q}_{i2}$ with values of $\mathbf{k}_f$ inferred from Mattheiss' calculations. The above proximity in points is reassuring, but sections **ΓK** and **ΓM** only were available in the calculations and no errors in either data are shown. As such, the detailed shape suggested by Scruby *et al.* [27] and later by Yamada *et al.* [28] requires examination as this departs from the simple ellipse proposed by Wilson *et al.* [2]. In fact, it is the form of the diffuse streaking in both electron and X-ray diffraction which suggests this shape. Assuming the critical Q_{i2} which produce strong reflexions $\{\mathbf{S}_M\}$ are not unique scattering vectors, general perturbations q_g (Fig. 12) might also be expected to give rise to divergent contributions in χ^0 **q** leading to a detectable phonon softening for certain modes. The diffuse scattering might therefore be interpreted as an image of the Fermi surface provided that χ^0 **q** (or more properly χ**q**) peaks close to wave vectors characterising its undistorted geometry (Freeman *et al.* [29] ; Fehlner and Loly [30]). This begs the question regarding the precise nature of the scattering which, as we have pointed out above, is predominantly transverse in character, and may, we conjecture, represent a dynamic effect.

The inflected, *dumb-bell* shape is, furthermore, consistent with Wilson *et al.* ; suggestions regarding nesting of this Fermi surface for the critical vector $\mathbf{Q}_i$. As those authors correctly point out for the unphysical case of a parallel, flat sided Fermi surface (Fig. 14*a*), the $\mathbf{Q}_i$ adopted, parallel to **M** maximises nesting of all six segments of Fermi surface, whereas the other possibility, parallel to **ΓK** (14*b*) couples only two segments effectively. Unfortunately, as is seen in figure 14*c*, an elliptical cross section, of any significant curvature close to the zone boundary, destroys much of the nesting of figure 14*a*. Only for the proposed *dumb bell* shape is effective nesting restored for $\mathbf{Q}_i \parallel \mathbf{\Gamma M}$. We note further that such a geometry results in points of inflexion close to the critical, spanning $\mathbf{Q}_i$, with, therefore, large local radius ($\rightarrow \infty$) again a situation favouring a divergent χ^0 **q**.

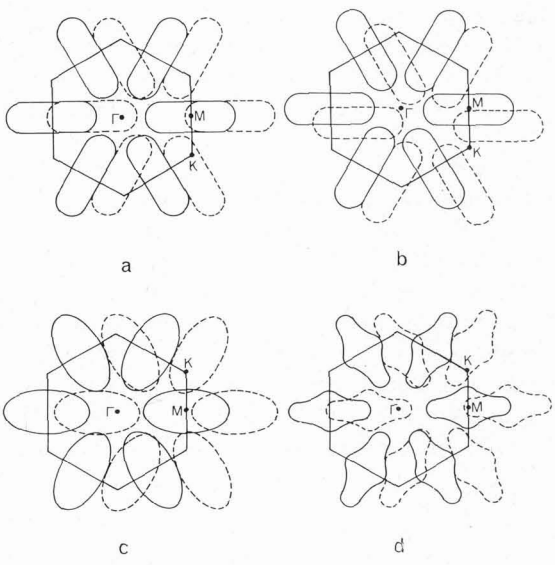

FIG. 14. — (*a*) Demonstrating superior nesting of all six segments of Fermi surface for spanning vector $\mathbf{Q}_i$ parallel to ΓM for an idealized flat sided surface, compared with (*b*) nesting of only two segements of same surface for vector parallel to ΓR. (*c*) Elliptical Fermi surface showing how good nesting of (*a*) is destroyed by curvature of surface (*d*) shape of surface in figure 13 proposed from image in diffuse scattering showing again how good nesting results for $\mathbf{Q}_i$ parallel to ΓM.

Following intercalation, as discussed above, or substitutional doping, the size of the critical spanning vector is clearly linked to the carrier density of the material, as is conclusively demonstrated for Ti in 1 T-TaS_2 (Wilson *et al.* [2]). Alkali metal (or rare earth) intercalation somewhat predictably increases the magnitude of the spanning vector, consistent with donation of the outer « s » electron to the « d » band of the TMD and an expansion in the size of the Fermi sur face. The adoption of $\mathbf{Q}_{in} = \pm\ \mathbf{a}^*/3$ representing an increase from 0.285 $\mathbf{a}^*$ to 0.333 $\mathbf{a}^*$ in the size of the spanning vector at room temperature suggests a transfer of less than one electron per formula unit, consistent with the proposal (Clark *et al.* [25]) that the intercalate actually forms an ordered $\sqrt{3} \times \sqrt{3}$ lattice ($\frac{1}{3}$ alkali metal atom per formula unit). More surprising is the adoption at room temperature of a second, competing CDW, characterised by $\mathbf{Q}_i = \pm\ (2\,\mathbf{a}^* \sqrt{3})/9$, although this gives way to the 3 × 3 structure at low temperature. Certainly, we would anticipate that the introduction of charged ionic arrays on the interlamellar space would increase the three dimensional interactions along $\mathbf{c}^*$, leading to a greater degree of band dispersion and hence the possibility of spanning vectors with different components $\parallel \mathbf{c}^*$. For 4 Hb-TaS_2, two, independent, uncoupled CDW/PLD systems exist in differing layers of the structure in real space. Here, however, we appear to have the reciprocal space analogue of this with two independent CDW's supported by the same Fermi surface. Closer investigations of these interactions between CDW/PLD states and intercalation should prove fruitful.

Electronically, the consequences of the forgoing, namely the adoption of a CDW/PLD ground state (in pristine or intercalated material), are the destruction of large areas of nested Fermi surface by energy gaps. In this context, we note (Scruby, 1976) that for both 1 T_2 and 1 T_3-TaS_2, not only the $\mathbf{Q}_{in}$ for $\mathbf{S}_M$ (10.*l*) span the surface but also those for second order perturbations $\mathbf{S}_M$ (11.*l*). As such reflexions are *not* to be regarded as simple second order satellites of the $\mathbf{S}_M$ (10.*l*), but in fact represent distinct soft modes of different character, they also may give rise to gaps at the Fermi surface. On adoption of the $\sqrt{13}$ superlattice in 1 T_3, therefore, much, if not all, of the surface might conceivably be destroyed, consistent with the resistivity data below 190 K. This does not explain the metallic decrease in resistivity for 1 T-$TaSe_2$ (Wattamaniak *et al.* [20]).

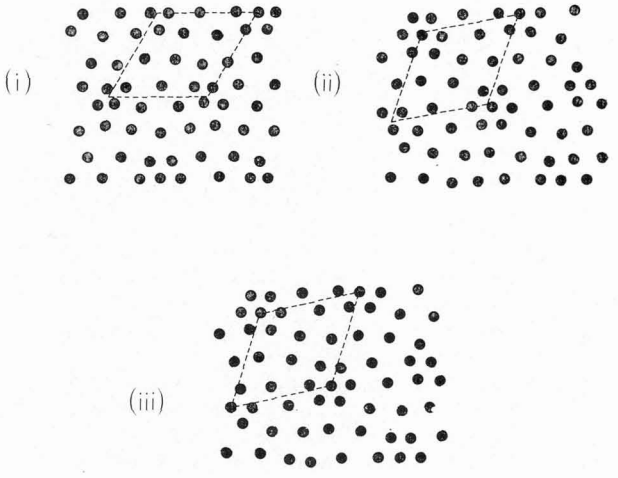

FIG. 15. — Model for single layer of Ta atoms in each distorted phase of 1 T-TaS_2 (for an arbitrarily large $U_Q \sim 0.1$ Å). Origin of distortion cell (Broken lines) arbitrary in the incommensurate 1 T_1 and 1 T_2 phases, and at a metal site in the commensurate 1 T_3 phase.

Finally we note that the question of the relative phases of the symmetry related CDW's within individual lamellae of the CDW/PLD ground state lattices has yet to be considered. This has been discussed in detail by Scruby *et al.* [1] and by Wilson *et al.* [2] and for the present purposes, we will confine ourselves to a brief review of the consequences of these phase relationships. Of initial interest are the relative phases of the CDW and PLD within individual layers. These may most logically be considered to be in phase, since this results in an overlap between regions of high ion core *and* conduction electron density, optimising screening of the potentials set up by the CDW. Having suggested that, however, it is the three dimensional elastic and coulomb interactions between neighbouring layers and between the symmetry related CDW/PLD's in each individual layer which determine the final form of the structure. The adoption of the 3 c o rhombohedral repeat in the PLD stacking in the incommensurate 1 T and 1 T_2 phases is an expression of this, the interlayer

interactions being minimised, as discussed elsewhere (Scruby *et al.* [1] ; Wilson *et al.* [2]). In real space however, it is the relative phases of the PLD's within the single layer which produce the result of most immediate physical significance. Thus, figure 14 illustrates a modulated matrix structure for the three phases of 1 T-TaS_2 for an arbitrary distortion amplitude and for three waves whose nodes coincide. In the incommensurate case (1 T_1, 1 T_2), the choice of origin is arbitrary, but in the commensurate 1 T_3 phase, this has been chosen to coincide with a metal atom site. For all three phases, particularly 1 T_3, the clutering of metal atoms around the CDW/PLD *Supercell* corners is evident, resulting in a reduced metal-metal overlap in the regions between. The strong resemblance between this situation and the conditions required for a Mott — type metal — insulator transition deriving from reduced metallic overlap form a tempting speculation with which to conclude the present discussion.

4. **Summary and acknowledgments.** — Concise summary of the above is difficult. This purely structural discussion omits references to the wealth of physical consequences of these charge density wave driven transitions, such as are reviewed elsewhere in the present volume. Final judgement on the above effects is therefore left to the reader, and we will conclude by thanking our Colleagues A. D. Yoffe and A. J. Grant for stimulating discussions.

References

[1] Williams, P. M., Parry, G. S. and Scruby, C. B., *Phil. Mag.* **29** (1974).
Scruby, C. B., Williams, P. M. and Parry, G. S., *Phil. Mag.* **31** (1975).

[2] This data is taken from
Wilson, J. A., di Salvo, F. J. and Mahajan, S., *Adv. Phys.* **24** (1975), 117 and is in fact a composite of references [4, 5] and [6].

[3] Wilson, J. A. and Yoffe, A. D., *Adv. Phys.* **18** (1969) 193.

[4] Thompson, A. H., Gamble, F. R. and Revelli, J. F., *Solid State Commun.* **9** (1971) 981.

[5] Thompson, A. H., Pisharody, K. R. and Koehler, R. F., *Phys. Rev. Lett.* **29** (1972) 163.

[6] Di Salvo, F. J., Bagley, B. J., Voorhoeve, J. M. and Waszczak, J. V., *J. Phys. Chem. Solids* **34** (1973) 1357.

[7] Mattheiss, L. F., *Phys. Rev.* B. **8** (1973) 3719.

[8] Shepherd, F. R. and Williams, P. M., *J. Phys.* C. *Solid State* **6** (1973) L 36, *ibid.* **7** (1974) 4416.

[9] Comes, R., Lambert, M., Laundis, H. and Zeller, H. R., *Phys, Rev.* B. **8** (1973a), 571 ; *Phys. Stat. Sol.*, B **58** (1973b) 587.

[10] Peierls, R. E., *Quantum Theory of Solids* (Oxford : Clarendon Press), 1955.

[11] Kohn, W., *Phys. Rev. Lett.* **2** (1959) 393.

[12] Brockhouse, B., *Phys. Rev. Lett.* **7** (1961) 93.

[13] Overhauser, A. W., *Phys. Rev.* **128** (1962) 1437 ; *Ibid.* **167** (1968) 692 ; *Ibid.* **133** (1971) 3173.

[14] Di Salvo, F. J., Wilson, J. A., Bagley, B. G. and Waszczak, J. V. *Phys. Rev.* B **12** (1975) 2220.

[15] Williams, P. M., Scruby, C. B. and Tatlock, G. J., *Solid State Commun.* **17** (1975) 1197.
Monckton, D. E., Axe, J. D. and di Salvo, F. J., *Phys. Rev. Lett*, **34** (1975) 734.

[16] Barmatz, M., Testardi, L. R., Disalvo, F. J., *Phys. Rev.* B **12** (1975) 4367.

[17] Ehrenfreund, E., Gossard, A. C., Gamble, F. R. and Geballe, T. H., *J. Appl. Phys.* **42** (1971) 194.

[18] Valic, M. I., Abdolall, K., Williams, D. L., Colloque Ampere, Nottingham 1974.

[19] Berthier, C., Jerome, D., Molinie, P., Rouxel, J., *Solid State Commun.* **19** (1976) 131.

[20] Wattamaniak, W. J., Tioman, J. P., Frindt, R. J., *Phil. Mag.* to be published.

[21] Di Salvo, F. J., Moncton, D. E., Wilson, J. A., Mahajan, S., *Phys. Rev. Lett.* to be published.

[22] Tatlock, G. J., *Commun. Phys.* **1** (1976).

[23] McMillan, W. L., *Phys. Rev.* B **12** (1975) 1187.

[24] Acrivos, J. V., Liang, W. Y., Wilson, J. A. and Yoffe, A. D., *J. Phys.* C. **4** (1971) L 18.

[25] Clark, W. B. and Williams, P. M., *Phil. Mag.* (1976) to be published.

[26] James, R. W., *The Optical Principles of the Diffraction of X-rays* (London : Bell), 1948.

[27] Scruby, C. B., Proceedings EMAG (1975), ed. Venables, J. A.

[28] Yamada, Y., Tsang, J. C. and Subba-Rao, G. V., *Phys. Rev. Lett.* **34** (1975) 1389.

[29] Freeman, A. To be published.

[30] Fehlner, W. R. and Loly, P. D., *Solid State Commun.* **14** (1974) 653.

[31] Smith, N. V., Traum, M. M. and di Salvo, F. J., *Solid State Commun.* **15** (1974) 211 ; *Phys. Rev. Lett.* **32** (1974) 1241.